Author/s:
Lee, J;Hill, A;Kentish, S

Title:
Formation of a thick aromatic polyamide membrane by interfacial polymerisation

Date:
2013-02-05

Citation:
Lee, J., Hill, A. & Kentish, S. (2013). Formation of a thick aromatic polyamide membrane by interfacial polymerisation. Separation and Purification Technology, 104, pp.276-283. https://doi.org/10.1016/j.seppur.2012.11.015.

Persistent Link:
https://hdl.handle.net/11343/324542

Formation of a thick aromatic polyamide membrane by interfacial polymerisation

Judy Lee[1], Anita Hill[2] and Sandra Kentish[1*]

1. Particulate Fluids Processing Centre, Chemical and Biomolecular Engineering, University of Melbourne, Parkville, Victoria 3010 Australia

2. Materials Science and Engineering, CSIRO, Clayton South, Victoria 3169, Australia

*sandraek@unimelb.edu.au

Abstract

Thin film composite membranes (TFC) consist of a thin film of polymer that is responsible for high salt rejection. This layer is made via interfacial polymerisation of two monomers 1,3 phenylene diamine and trimesoyl chloride, with the membrane has been reported to reach a self limiting thickness of less than 200 nm. This paper reports for the first time the formation of thick free-standing aromatic polyamide membranes of greater than 50 micron in thickness via the well-known interfacial polymerisation technique. The membrane thickness as a function of polymerisation time and monomer concentration was investigated. The polyamide layer formed through interfacial polymerisation is not necessarily homogeneous, but can indeed feature areas of porosity. A mechanism for such a porous structure is proposed and discussed. The ability to form thick free-standing polyamide membranes allows bulk polymer properties to be evaluated for the first time. In particular, in this work we are able to measure the zeta potential of the membrane surface that usually faces the membrane support. We show that this surface is still negatively charged for all pH values above 4.0.

Keywords: reverse osmosis, nanofiltration, interfacial polymerisation, porosity

1. Introduction

In the early 1980s John Cadotte [1-3] pioneered the fabrication of thin film composite (TFC) membranes using an interfacial polymerisation (IP) process. These membranes consist of a thin film of polymer resting on top of a porous support. It is this polymer film that is responsible for the high salt rejection and water flux properties of a TFC membrane, making it superior compare to other membranes for application of desalination and water purification.

The IP process, as its name suggests, occurs at the interface between two immiscible solvents that have been brought into contact. The polymerisation process involves the reaction between two monomers, usually a diamine in the aqueous phase and a dichloride in the organic phase [4]. Morgan et al. [4] have shown that the reaction predominantly occurs by the diffusion of diamines from the aqueous phase into the organic phase. This is due to the greater solubility of the amine in the organic phase compared to the dichloride solubility in water [4, 5]. However, commercial TFC membranes are usually made from the monomers 1,3 phenylene diamine (MPD) and a trichloride, trimesoyl chloride (TMC) [6-8]. The use of a trichloride increases the degree of cross-linking as initially the two monomers react to form linear chains as with the dichloride; while the third acyl chloride group can either undergo hydrolysis to form carboxylic acid or react with another diamine molecule to produce chain branching or cross-linking [9]. The additional carboxyl group allows for a greater degree of cross-linking and when left unreacted, adds a mild anionic charge to the membrane at neutral pH. All this gives rise to a superior membrane for salt rejection compared to linear polyamide 610 films that have been shown to be readily permeable to inorganic salts [4].

The formation of the interfacial polymer film is almost instantaneous and hinders the diffusion of the diamine monomers across the film, which inherently limits film growth [4]. The film formed during the initial period is said to form a smooth seal at the interface which hinders the subsequent diffusion of the diamines across to the organic phase [5]. It is the diffusion limited growth towards the organic phase which gives rise to the rough morphology on the surface facing the organic phase that is often reported [4, 10, 11]. This morphology is often referred to as a ‘ridge and valley’ structure [4, 10, 11] or as a surface covered with ‘protuberances’ [12]. Recent work by Kimura et al. [13] has shown that these protuberances may be hollow, providing additional membrane area for water transport, but altering our perception of how the active layer forms.

Chai et al.[14] used light reflection and pendant drop tensiometry to investigate the kinetics of the film formation process. They found the reaction between MPD and TMC monomers to be very fast and self limiting in only a few minutes. The concentration of TMC and the reaction time did not have a significant effect on the film thickness, which varied between 0.1- 0.5 μm. Contrary to these findings, Roh et al. [15] reported an increase in the film thickness from 0.1 - 0.5 μm when the TMC concentration increased from 0.01-1 w/v% for a given MPD concentration. A smaller increase was observed with increasing MPD concentration for a given TMC concentration. Several mathematical models describing the film growth have been proposed [5, 16], however, the polymerisation between MPD and TMC is so fast and the resulting film is so thin such a direct comparison of the model with that of experimental data have not been possible. This implies that only very thin films ever form.

The fragility of this ultra-thin, non-porous layer creates a challenge to the understanding of the bulk properties of the layer. In turn, this limits the ability to develop good models of salt and water transport. As one example, common models for salt transport assume that the membrane charge is uniform throughout the bulk of the active layer [17, 18]. However, this assumption is not readily validated because only the charge on the top surface can be measured. This paper will demonstrate for the first time the synthesis of thick aromatic polyamides that can be readily handled. The ability to form thick free-standing polyamide membranes allows the membrane charge on the underside of the active layer to be evaluated, which would otherwise be difficult if the active layer was 200 nm or thinner. The salt permeability of these membranes is also presented and related to the changing structure of the membrane with time. These results increase our understanding of how the active layer is formed and will thus be important for the future development of novel TFC membrane structures. Results will also assist with the modelling of salt and water transport through the layer structure.

2. Experimental method

2.1 Membranes and chemical reagents

Commercial polyamide membranes BW30LE and SW30 were kindly supplied by Dow Filmtec. Porous polysulfone membrane support was kindly supplied by GE Water. N,N-dimethyl formamide (DMF) (98 %, Chemsupply), 1,3-phenylenediamine (MPD) (99+ %, Aldrich), trimesoyl chloride (TMC) (98 %, Aldrich), sodium chloride (NaCl) (99 %, Chemsupply) calcium chloride ($CaCl_2$) (98+ %, Merck) and n-hexane (95 %, BDH) were used as received.

2.2 Membrane synthesis

(a) TFC membranes

In situ-prepared thin film composite membranes were made by interfacial polymerization [2]. GE polysulfone was soaked in a solution of 2 % w/v MPD in water for 15 min. The excess MPD solution was removed from the surface of the polysulone support before immersing in a solution of 0.1 % w/v TMC in hexane. The contact time for the interfacial reaction was 10 seconds. The membrane was then washed with hexane to removed any excess TMC, followed by Milli-Q water for the removal of any excess MPD. The membrane was then kept in Milli-Q water.

(b) Free standing thick polyamide membranes

The aqueous phase consisted of 2 w/v% of MPD in water and for the organic phase, a concentration range of TMC in hexane between 0.01 and 0.1w/v % was used. The interfacial polymerization process was performed in a cylindrical cell with a diameter and height of 4 cm and 5.5 cm, respectively. 15 mL of aqueous phase was first poured in to the cell. A funnel was then carefully positioned over the top of the aqueous phase near the edge of the cell to allow 40 mL of the organic phase to gently cover the top surface of the aqueous phase. This method of introducing the organic phase was fixed to ensure that all samples had the same initial interfacial polymerisation conditions. A volume of 40 mL was chosen to ensure there was a sufficient volume of liquid in the cell and to minimise any evaporation of the volatile hexane over the course of the interfacial polymerisation time. This evaporation was

further minimised by sealing the cell. The reaction was left undisturbed for a predetermined number of days before the polymer film was collected and washed repeatedly with ethanol and water.

2.3 Field Emission Scanning Electron Microscope (FESEM)

The surface and cross-sectional structure of the aromatic polyamide films were imaged using a Philips XL30 FEG FESEM. For the cross-sectional structure, the membranes were carefully cut with a very sharp razor and tilted by 90 degrees. All samples images were sputter-coated with gold under vacuum prior to imaging.

2.4 Salt diffusion experiments

A diffusion cell from Permgear was used to perform direct osmosis experiments. The setup is depicted in Figure 1. It consisted of a two compartment cell design, with each compartment having a volume of 3.4 mL and an orifice diameter of 0.5 cm. The membrane was sandwiched between two teflon gaskets and clamped between the two compartments. One compartment (receiver cell) was filled with Milli-Q water whereas the other compartment (donor cell) was filled with electrolyte solution. The solutions were stirred at a rate of 700 rpm to reduce external concentration polarization and the porous paper layer was removed from TFC membranes to reduce internal concentration polarization. Agreement between the mass transfer coefficient obtained experimentally for BW30LE and that calculated from the manufacturer specifications (see Section 3 below) confirmed that such concentration polarisation was minimal. Cooling water was used to maintain the temperature of the solutions at 25 ^{o}C. The conductivity of the solution in the receiver cell was recorded as a function of time using a conductivity probe, and the conductivity converted to salt concentration via a calibration curve.

The mass transfer coefficient or permeability constant was calculated using Equation 1 [19]:

$$-\frac{V}{2A}\ln\left(1-\frac{2C_R(t)}{C_D(0)}\right)=\boldsymbol{k_{ov}}t \qquad [1]$$

$$k_{ov} = \frac{P}{l} \qquad [2]$$

Where $C_R(t)$ is the salt concentration in the receiver cell at time t, $C_D(0)$ is the initial salt concentration in the donor cell, V is the volume of solution in each cell, A is the membrane area and K_{ov} is the overall salt mass transfer coefficient or salt permeance. It should be noted that both the mass transfer coefficient and the permeability represent the total permeation through the membrane. In a porous membrane these values can be related to both rapid transport of salt through the pores and much slower transport through the polymer material itself.

The derivation of this equation from Fick's first law of diffusion assumes constant volume in both of the compartments. A low salt concentration of 2 g/L was used to reduce the water transport induced by osmosis. At this salt concentration the water flux was calculated to be approximately 0.11 mL/hr for BW30LE using the water permeance of 1.02×10^{-8} L/m^{2}sPa given by the manufacturer [20]. This accounts for approximately 4 % change in the volume of solution used (2.8 mL) in one hour. It is thus assumed that the water transport induced by osmosis is insignificant. Experimentally, the curve of concentration as a function time has an initial delay as the salt diffuses through the membrane and becomes linear for up to three hours. This allows Equation 1 to be fitted and K_{ov} to be evaluated from the gradient of the linear region. For homogeneous and dense membranes, the salt mass transfer coefficient in Equation 1 can be defined by Equation 2 as the salt permeability (P) divided by the thickness of the membrane (l).

2.5 Zeta potential

An electrokinetic analyser (EKA) from Anton Paar GmbH, Austria was used to measure the zeta potential of the aromatic polyamide film. Two pieces of the film was mounted face to face in a rectangular cell. A PTFE spacer was used to create a flow channel with an effective area of 735 mm^2 between the membranes. The potential difference between both ends of the cell was measured using two reversible Ag/AgCl electrodes. A background electrolyte of 1 mM sodium chloride was used and the solution pH was adjusted from 3 to 10 using 0.1 M hydrochloric acid and 0.1 M sodium hydroxide, respectively. Experiments were conducted at a constant temperature of 25 ˚C. The Helmholtz-Smoluchowski equation with Fairbrother and Matsin substitution was employed to generate zeta potential values [21].

Due to the larger surface area required for the zeta potential analysis, the polyamide film was formed in a covered larger cell with a diameter and height of 19 cm and 9 cm, respectively. It was found that when a larger cell was used, for a given reaction time, the film appeared thinner than that synthesised in a smaller cell. This difference in the thickness might be attributed to differences in the flow of the organic phase over the top of the aqueous phase. Since the interfacial polymerisation is almost instantaneous, the way the two fluids are brought into contact will be important. This will affect the formation of the initial membrane barrier and the mass transfer of solutes through this layer, which subsequently affects the growth of the membrane as a function of time. However, these differences in thickness should not affect the charge of the cross-linked surface facing the aqueous side.

3. Results and Discussion

3.1 Active layer from thin film composite membrane

Height images and topography profiles of the surfaces of the active layer from a commercially available SW30 membrane were obtained using AFM. The upper surface of the active layer, which is the side facing the organic phase during the interfacial polymerisation process, reveal a rough peak and valley structure that has often being reported by others [4, 10, 11, 22-26] for aromatic polyamide TFC membranes (Figure 2 (a)). The underside of the active layer (Figure 2 (b)), the side facing the aqueous phase during interfacial polymerisation process, appears to be smoother than the upper surface. This is evident in the surface topography profiles present for the two surfaces. The top surface of a GE porous polysulfone membrane support was also imaged (Figure 2 (c)) and is relatively flat in comparison with either surface of the active layer. The surface roughness for the three surfaces was validated quantitatively. For the upper and underside of the active layer, the surface RMS roughness was 84 nm and 38 nm, respectively and for the polysulfone support, a surface RMS roughness of 3.5 nm was measured.

Shown in Figure 3 is a SEM image of a folded sheet of unsupported aromatic polyamide isolated from the SW30 membrane showing a thickness of around 0.16 ± 0.02 μm. It is known that the thickness may vary depending on the location and we have found the thickness to vary between 0.14 to 0.23 μm. This is within the range reported in the literature

for aromatic polyamides (0.20 - 0.30 μm) [6, 27]. For BW30LE, a membrane thickness of between 0.07-0.14 μm was measured. The exact composition and reaction time used by the manufacturer is not known, however a polymer film made in-house using 2 w/v % MPD and 0.1 w/v % TMC with a reaction time of 10 seconds produced a comparable thickness of around 0.09 - 0.14 μm. Again, the top surface of the polyamide is rough and rugged and the underside of the polyamide appears smooth, which is consistent with the AFM analysis above. A closer examination of the underside revealed small pores, which supports Cadotte's claim that the back surface of the barrier layer is highly porous, allowing the amine-migration mechanism to take place [9]. The presence of these pores is also consistent with the recent finding that the protuberances present on the top surface of the active layer are hollow [13]. The pores could represent entrances into these protuberances.

3.2 Thick aromatic polyamide

The surfaces and cross-section of thick polyamide films, prepared in-house by extending the film reaction time to greater than one day, are depicted in Figure 4. The polyamide film shows both a rough and smooth surface, similar to that observed for the commercial polyamide shown in Figure 3. A similar porous structure on the underside of the film is also evident (Figure 4b). However, somewhat unexpectedly, the cross-section of this thick polyamide layer also appears very porous (Figure 4c). This differs from the dense, non-porous barrier layer that has been associated with TFC membranes.

The non-uniform and porous thick active layer supports the recent report by Freger et al. [5, 28] that the active layer of the TFC membranes is less homogeneous and that the polymer density is unevenly distributed across the thickness of the membrane. The growth of porous structures has been demonstrated with other interfacial polymerisation systems involving an aliphatic triamine with an aromatic chloride [29] and aliphatic diamines with a disulfonyl chloride [30]. However, these polymer films exhibited a much more porous cellular structure compare to the membranes formed in this study. Jansen et al. [29] attributed the large spherical pores that are created in their system to the formation of aqueous droplets on the surface facing the organic phase, which they observed directly using light transmission microscopy. These authors argued that the polymer film is swollen with the aqueous phase and as more polymer forms, this water is expelled into the organic phase. As time progresses, the small water droplets coalesce to form larger ones, leading to the larger cavities that occurred within their films over time. In the case of MPD and TMC, it is possible that similar

water droplets are formed in the organic phase to cause the porous structure. It is proposed that at first the interfacial polymerisation is fast and a thin film is formed at the interface (Figure 5(a)). This film is swollen with water, and as time passes, some water is expelled into the organic phase forming small droplets on this side (Figure 5(b)). MPD, which is larger than water molecules, would permeate slower than water and will subsequently diffuse from the aqueous phase through this interfacial layer into these water droplets (Figure 5(c)). This will initiate interfacial polymerisation at the new interface. Therefore, over a period of time a porous structure will develop. This is supported by a closer examination of the layer beyond the initial film barrier (Figure 6(a)) which shows the surface of the polyamide facing the MPD solution with a portion of the subsurface exposed. There is evidence of spherical pockets, possibly formed by such water droplets. Figure 6(b) is a closer look at the barrier layer, which further supports the explanation of the initial diffusion of the water through the interfacial layer to create a new aqueous/organic interface.

3.3 Polymerisation reaction time

Figure 7 shows the effect of increasing the interfacial polymerisation time on the film thickness when the MPD and TMC concentrations were fixed at 2 w/v % and 0.1 w/v %, respectively. It is known the reaction between MPD and TMC is fast and a dense film is formed almost instantaneously upon contact of the two solutions. Chai et al. [14] reported the initial film to reach a self limiting thickness after 10 seconds for the concentrations similar to that used in this study. This initial self limiting thickness can be seen in Figure 7 at reaction times less than one day where very little change in the film thickness was observed. It is always accepted that the self limiting thickness occurs due to the resistance to diffusion of MPD through this layer. However, Figure 7 demonstrates that further increase in the reaction times beyond a day resulted in a steady growth in the film thickness. It is possible that after the formation of the initial polymer barrier (Figure 5(a)) some time is required for water to be expelled from the polymer membrane (Figure 5(b)). The presence of water on the organic side creates new surfaces for interfacial polymerisation to occur. The increase in the available surface for interfacial polymerisation triggers the growth in the film thickness observed after one day. It is also possible that the polymer layers formed after the initial barrier have a lower cross-linking due to a lower concentration of MPD, thus making them

more permeable and thus more readily able to provide the necessary reagents for new surface to form and increase the membrane thickness.

3.4 Salt Permeation

The salt permeability and mass transfer coefficient of the membranes was measured using the diffusion cell. The measurement protocols were first validated by testing a sample of commercial BW30LE membrane. The mass transfer coefficient obtained (1.64 x 10^{-5} cm/s) was comparable to that calculated from the manufacturer specifications (1.3 x 10^{-5} cm/s) [20] confirming the accuracy of the technique. A polymer film made in-house using 2 w/v % MPD and 0.1 w/v% TMC with a reaction time of 10 seconds produced a comparable salt mass transfer coefficient of 1.71 x 10^{-5} cm/s.

With increasing polymerisation time (or increase in membrane thickness) the salt mass transfer coefficient decreases, whereas an increase in the permeability is observed (Figure 8). The salt mass transfer coefficient is inversely proportional to the membrane thickness, and therefore is expected to decrease with increasing thickness as observed. Conversely, the permeability is independent of membrane thickness (Equation 2). As discussed above, such a permeability in a porous membrane is representative of both rapid transport through pores and a much slower transport through the polymer material. The SEM images at longer polymerisation times clearly show a non homogenous membrane with areas of high porosity. Thus salt permeability probably increases because of increases in overall porosity with time, rather than any increase in the permeability of the intrinsic polymer material itself. The permeability appears to stabilise or even decrease after three days of reaction; however such changes are within the range of experimental error.

3.4 TMC concentration

The relationship between the TMC concentration and film thickness at a fixed MPD concentration of 2 w/v % and reaction time of 2 days is plotted in Figure 9 and the corresponding salt permeability and mass transfer coefficient is given in Figure 10. With increasing TMC concentration (or increasing -COCl/-NH3 ratio) the thickness of the polymer film increases, the mass transfer coefficient decreases slightly whereas the permeability is observed to increase. This result contradicts that reported by Roh et al. [15] where an increase in salt rejection and decrease in water flux was observed for TFC membranes

synthesised with increasing TMC concentration. The membranes investigated by Roh et al. [15] were thin, dense polyamides formed on top of a support layer in a very short polymerisation time, whereas in this study the polyamide layers were thick and porous, and were investigated without any supporting layers.

SEM images of the polymer film made at different TMC concentrations are pictured in Figure 11. The increase in the film thickness is clear in the top images of Figure 11, however the porosity of the sublayer appears denser for the thicker film, which does not explain the higher salt permeability. The bottom images in Figure 11 show the underside of the polymer film that is facing the MPD aqueous solution. At a TMC concentration of 0.01 w/v % very few pores are present, but the surface appears to show crater like indentations. With increasing TMC concentration the pores appear to be more prominent and deeper.

As mentioned earlier, the permeability of amine becomes limited once the initial polymer barrier is formed and the slow diffusion of amine through this barrier layer limits further reaction with the TMC in the organic phase. One can conclude that a thinner film obtained at low TMC concentrations is the result of the formation of a very dense initial polymer barrier (as seen by a non porous surface in Figure 11) which lowers the extent to which amine and water can diffuse through to further react with the TMC in the organic phase. Similarly, the porous structure observed at high TMC concentrations resulted in a thicker film as the initial dense barrier is more permeable to the diffusion of amines. The resistance to the diffusion of amines is reflected in the mass transfer coefficient of salt shown in Figure 10.

One possible explanation for the increase in the porosity of the initial polymer barrier at higher TMC concentrations could be the hydrolysis of the active acid chloride end groups [31]:

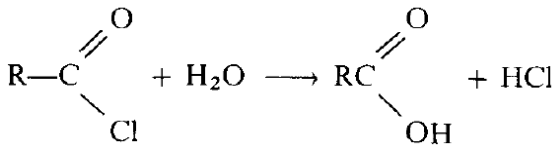

The formation of the carboxylic acid end group will block reactions with the diamines and prevent further polymerisation to occur. Since the MPD concentration is fixed at 2 wt %, with increasing TMC concentration from 0.01 wt % to 0.1wt %, the molar ratios of TMC to MPD varies from 2 to 20, respectively. Therefore, more hydrolysis of the acid chloride end groups is expected to occur at high TMC concentrations. In addition, higher TMC

concentration will also increase the rate of hydrolysis and the rate of interfacial polymerisation itself [32]. This could lead to uneven formation of the film barrier, leading to a more porous film.

3.5 Surface charge

The surface charge for a typical aromatic polyamide TFC is known to be negative across a broad pH range. However, this measurement is made on the side that is in contact with the organic phase. Shown in Figure 12 is the zeta potential as a function of pH for a commercial TFC membrane, BW30LE. Our previous work [7] has shown that this material is a standard polyamide membrane without any surface coating. The zeta potential is indeed negative at pH above 3.3. Due to the method by which commercial TFC membranes are manufactured and the thinness of the active layer, it is difficult to determine the surface charge on the side that is facing the aqueous phase (which is the side in contact with the polysulfone). With the thick polyamide developed here, it is possible to study the surface charge on the surface facing the aqueous phase. It can be seen in Figure 12 that the surface facing the MPD aqueous solution appears to be still negatively charged but slightly less positive compared to the side facing the organic phase. The isoelectric point moves to around 3.9, which means that both surfaces remain negatively charged across the pH range generally employed for these membranes. This result differs from that reported by Freger et al. [5] where they used staining and TEM to show the surface facing the organic phase was negatively charged and the surface facing the polysulfone was positively charged. The discrepancies may be attributed to the different techniques used. However, the present result validates the assumption of a relatively constant membrane charge that is currently used in the modelling of salt transport through these membrane systems [17, 18].

4. Conclusion

The results reported in this paper have significant implications concerning the formation mechanism of the active barrier in thin film composite membranes. Specifically, this work has shown that the polyamide layer formed through interfacial polymerisation is not necessarily homogeneous, but can indeed feature areas of porosity, possibly formed through the permeation of water through the membrane layers, or expulsion of water from the

polymer itself. The porous structure on the underside may possibly be related to the ridge and valley structure, or protuberances commonly observed on the top surface of the membrane. These results can be used to better understand how to alter the morphology of the active layer and thus how to change its intrinsic performance.

The ability to form thick free-standing polyamide membranes also allows bulk polymer properties to be evaluated for the first time. In particular, we have shown here that the side of the membrane facing the support remains negatively charged at most pH values, although the charge is less negative than on the top surface of the membrane. These results can be used to improve mathematical models for interfacial polymerisation processes.

Acknowledgements

The Authors acknowledge the Australian Research Council Discovery Projects Scheme (DP1093815) for their financial support. The Particulate Fluids Processing Centre, a Special Research Centre of the Australian Research Council is also acknowledged for infrastructure support. CMD and AJH acknowledge the support of CSIRO's Office of the Chief Executive Science Leader program.

References

[1] J.E. Cadotte, Reverse osmosis membrane, in: US Patent No. 4,039,440 (1977)
[2] J.E. Cadotte, Interfacially synthesized reverse osmosis membrane, in: US Patent No. 4,277,344 (1981).
[3] J.E. Cadotte, R.S. King, R.J. Majerle, R.J. Petersen, Interfacial synthesis in the preparation of reverse osmosis membranes, J. Macromol. Sci. Part A., A15 (1981) 727-755.
[4] P.W. Morgan, S.L. Kwolek, Interfcial polycondensation. II Fundamentals of polymer formation at liquid interfaces, J. Polymer Sci., 40 (1959) 299-327.
[5] V. Freger, S. Srebnik, Mathematical model of charge and density distributions in interfacial polymerization of thin films, J. Appl. Polym. Sci., 88 (2003) 1162-1169.
[6] R.J. Petersen, Composite reverse osmosis and nanofiltration membranes, J. Membr. Sci., 83 (1993) 81-150.
[7] A. Widjaya, T. Hoang, G.W. Stevens, S.E. Kentish, A comparison of commerical reverse osmosis membrane characteristics and performance under alginate fouling conditions, Separation and Purification Technology, 89 (2012) 270-281.
[8] J. Lee, M. Ashokkumar, K. Yasui, T. Tuziuti, T. Kozuka, A. Towata, Y. Iida, Development and optimization of acoustic bubble structures at high frequencies, Ultrason. Sonochem., 18 (2011) 92-98.
[9] J.E. Cadotte, Evolution of composite reverse osmosis membranes, in: D.R. Lloyd (Ed.) Materials science of synthetic membranes, ACS Symposium Series 269, American Chemical Society, Washington D.C., 1985, pp. 273-294.
[10] C.Y. Tang, Y.N. Kwon, J.O. Leckie, Probing the nano- and micro-scales of reverse osmosis membranes-A comprehensive characterization of physicochemical properties of uncoated and coated membranes by XPS, TEM, ATR-FTIR. and streaming potential measurements, J. Membr. Sci., 287 (2007) 146-156.
[11] S.Y. Kwak, S.G. Jung, Y.S. Yoon, D.W. Ihm, Details of surface features in aromatic polyamide reverse osmosis membranes characterized by scanning electron and atomic formce microscopy, J. Polymer Sci. Part B, 37 (1999) 1429 - 1440.
[12] T. Ogawa, M. Henmi, M. Kimura, H. Tomioka, T. Sasaki, M. Koiwa, Energy saving RO membrane based on scientific research, in, Pacifichem 2010, International Chemical Congress of Pacific Basin Societies, Honolulu, HI, United States, December 15-20, 2010 pp. MATNANO-388.
[13] M. Kimura, K. Nakatsuji, T. Sasaki, M. Henmi, Progress of RO Membrane Technology based on Scientific Research for Seawater and Brackish Water Desalination, Procedia Engineering, 44 (2012) 598-599.
[14] G.Y. Chai, W.B. Krantz, Formation and characterization of polyamide membranes via interfacial polymerization, J. Membr. Sci., 93 (1994) 175.
[15] I.J. Roh, A.R. Greenberg, V. Khare, Synthesis and characterization of interfacially polymerized polyamide thin films, Desalination, 191 (2006) 279-290.
[16] J. Ji, J.M. Dickson, R.F. Childs, B.E. McCarry, Mathematical model for the formation of thin-film composite membranes by interfacial polymerization: Porous and dense films, Macromolecules, 33 (2000) 624-633.
[17] S. Bandini, D. Vezzani, Nanofiltration modeling: The role of dielectric exclusion in membrane characterization, Chemical Engineering Science, 58 (2003) 3303-3326.
[18] W.R. Bowen, J.S. Welfoot, Modelling the performance of membrane nanofiltration—critical assessment and model development, Chemical Engineering Science, 57 (2002) 1121-1137.
[19] W. Jost, Diffusion in solids, liquids and gases, Academic Press, New York, 1960.

[20] M. Reali, G. Dassie, G. Jonsson, Computation of salt concentration profiles in the porous substrate of anisotropic membranes under steady pressure-retarded osmosis conditions, J. Membr. Sci., 48 (1990) 181-201.
[21] F. Fairbrother, M. Mastin, Studies in elecro-endosmosis part I, J. Chem. Soc., 125 (1924) 2319-2330.
[22] S.Y. Kwak, D.W. Ihm, Use of atomic force microscopy and solid-state NMR spectroscopy to characterize structure-property-performance correlation in high-flux reverse osmosis (RO) membranes, J. Membr. Sci., 158 (1999) 143-153.
[23] V. Freger, Swelling and morphology of the skin layer of polyamide composite membranes: An atomic force microscopy study, Environ. Sci. Technol., 38 (2004) 3168-3175.
[24] M. Liu, D. Wu, S. Yu, C. Gao, Influence of the polyacylchlroide structure on the reverse osmosis performance, surface properties and chlorine stability of the thin-film composite polyamide membranes, J. Membr. Sci., 326 (2009) 205-214.
[25] G. Hurwitz, G.R. Guillen, E.M.V. Hoek, Probing polyamide membrane surface charge, zeta potential, wettability, and hydrophilicity with contact angle measurements, J. Membr. Sci., 349 (2010) 349-357.
[26] A.K. Ghosh, B.H. Jeong, X. Huang, E.M.V. Hoek, Impacts of reaction and curing conditions on polyamide composite reverse osmosis membrane properties, J. Membr. Sci., 311 (2008) 34 - 45.
[27] in: DOW Water & Process Solutions Technical Manual, http://www.dowwaterandprocess.com/support_training/literature_manuals/filmtec_manual.htm.
[28] V. Freger, Nanoscale heterogeneity of polyamide membranes formed in interfacial polymerization, Langmuir, 19 (2003) 4791-4797.
[29] L.J.J.M. Janssen, K. te Nijenhis, Encapsulation by interfacial polycondensation. I. The capsule production and a model for wall growth, J. Membr. Sci., 65 (1992) 59-68.
[30] J. Ji, B.J. Trushinski, R.F. Childs, J.M. Dickson, B.E. McCarry, Fabrication of thin-film composite membranes with pendant, photoreactive diazoketone functionality, J. Appl. Polym. Sci., 64 (1997) 2381-2398.
[31] V. Enkelmann, G. Wegner, Mechanism of interfacial polycondensation and the direct synthesis of stable polyamide membranes, Makromol. Chem., 177 (1976) 3177-3189.
[32] A.L. Ahmad, B.S. Ooi, Properties-performance of thin film composites membrane; study on trimesoyl chloride content and polymerization time, J. Membr. Sci., 255 (2005) 67-77.

Figure Captions

Figure 1: Diffusion cell used in the osmosis experiment.

Figure 2: 5μm x 5μm AFM height images (top) and topography profile (bottom) of: (a) top surface of SW30 in dry state, (b) bottom surface of SW30 in dry state, and (c) top of the polysulfone support.

Figure 3: SEM image of the cross-sectional thickness of the active layer of a commercial membrane, SW30.

Figure 4: SEM image of (a) the top surface of the polyamide facing the organic solution (b) bottom surface of polyamide facing MPD aqueous solution and (c) cross-section of the polyamide. For (a) and (b), the polymer was synthesised with 0.1 w/v % TMC and 2 w/v % MPD and reacted for 6 days. For (c) the polymer was synthesised with 0.05 w/v % TMC and 2 w/v % MPD and reacted for 2 days.

Figure 5: An illustration of the mechanism of thick membrane formation: (a) initial thin membrane formation upon contact with the two solutions (b) slow diffusion of water through the membrane (c) diffusion of MPD through the membrane causing new membranes to form.

Figure 6: SEM images of (a) the surface facing the aqueous side with the subsurface exposed and (b) enlarged image of the cross-section of the film barrier facing the aqueous side.

Figure 7: Polymer film thickness as a function of polymerisation time. The MPD and TMC concentration was fixed at 2 w/v% and 0.1 w/v%, respectively.

Figure 8: Salt permeability (triangles) and salt mass transfer coefficient (squares) as a function of polymerisation time. The thick polyamide membranes were made with a fixed concentration of 2w/v% MPD and 0.1 w/v % TMC. The empty symbols are thin polyamides made on top of polysulfone supports, similar to commercial TFC membranes.

Figure 9: Polymer film thickness as a function of TMC as well as the -COCl/-NH_3 ratio. The polymerisation reaction time and MPD concentration was fix at 2 days and 2w/v%, respectively.

Figure 10: Salt permeability (■) and salt mass transfer coefficient (▲) as a function of TMC concentration as well as -COCl/-NH_3 ratio. The polymerisation reaction time and MPD concentration was fix at 2 days and 2w/v%, respectively.

Figure 11: SEM image of aromatic polyamide showing the cross-sectional thickness (top) and surface facing the MPD aqueous phase (bottom) synthesised with different concentrations of TMC: (a) 0.01 w/v % (b) 0.05 w/v % and (c) 0.1 w/v %. The aqueous phase was fixed at 2 w/v % MPD and the interfacial polymerization time was 2 days. In (a) the polyamide membrane is too thin to be self supporting and therefore for the cross-sectional image, the membrane is rested on top of a polyester support for imaging purposes.

Figure 12: Surface charge measurements for the membrane surface facing the MPD aqueous side (circle) and for the surface facing the TMC organic side (square), as a function of pH.

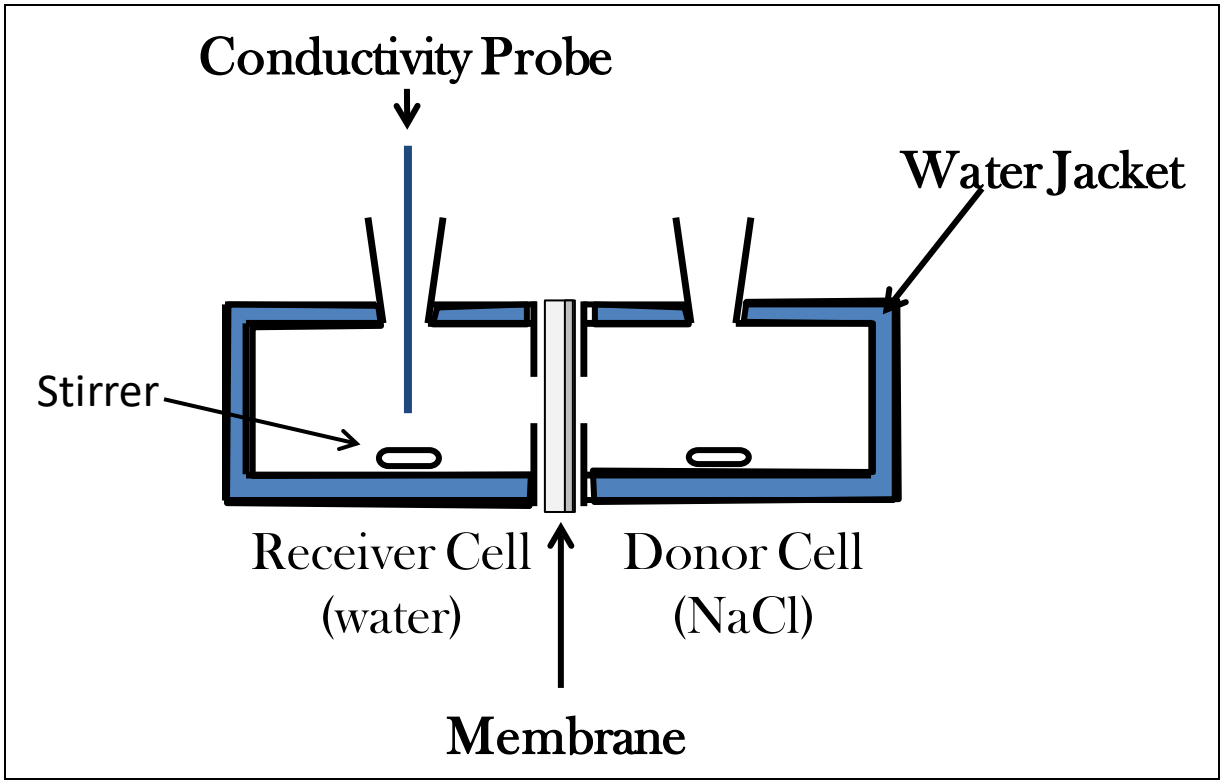

Figure 1: Diffusion cell used in the osmosis experiment.

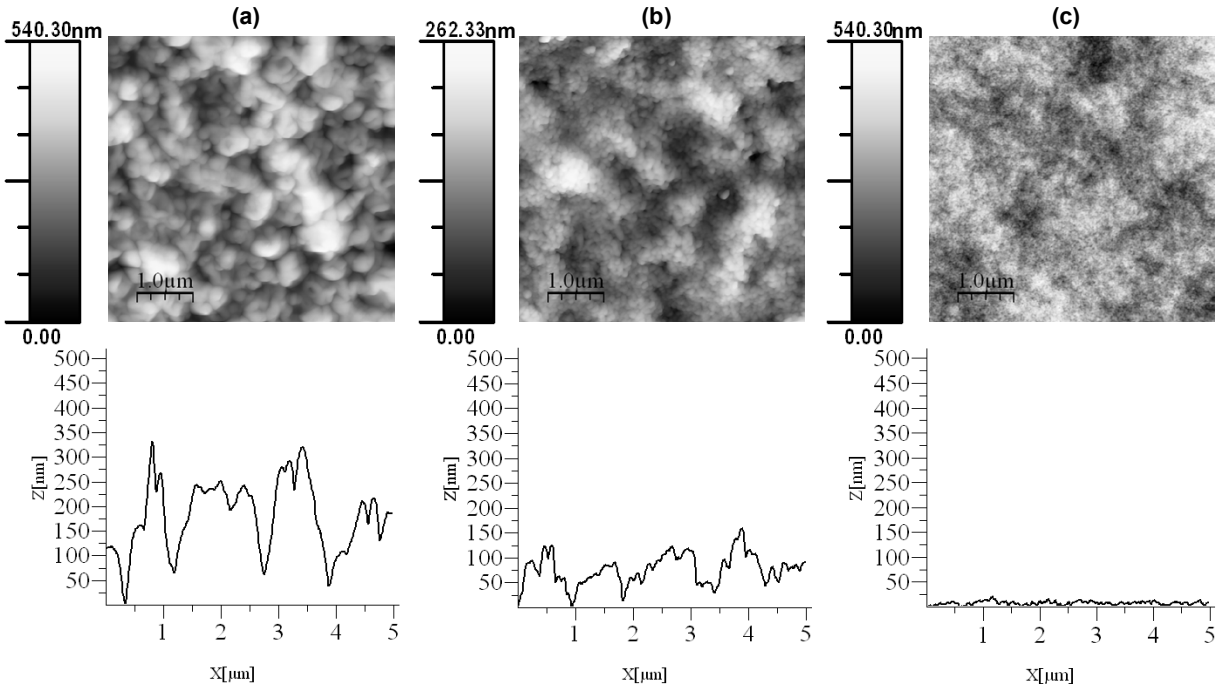

Figure 2: 5µm x 5µm AFM height images (top) and topography profile (bottom) of: (a) top surface of SW30 in dry state, (b) bottom surface of SW30 in dry state, and (c) top of the polysulfone support.

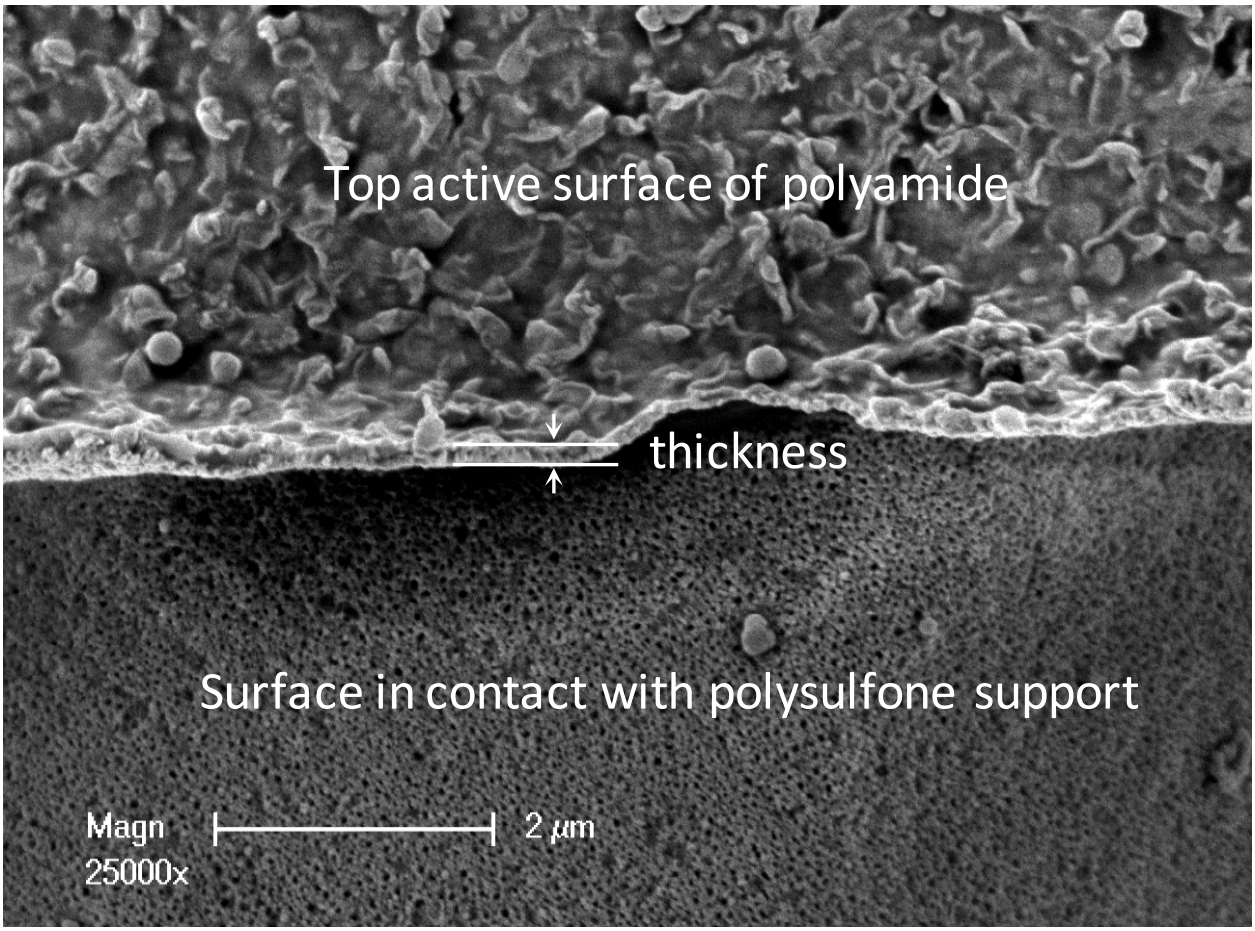

Figure 3: SEM image of the cross-sectional thickness of the active layer of a commercial membrane, SW30.

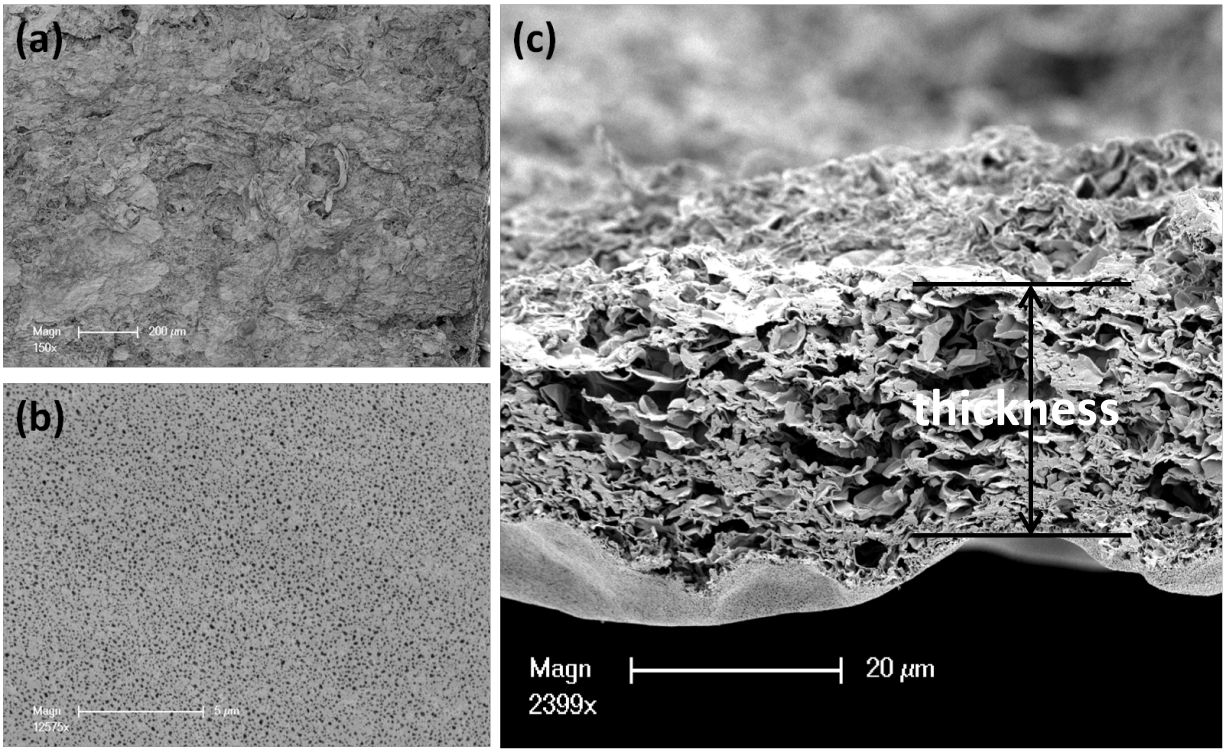

Figure 4: SEM image of (a) the top surface of the polyamide facing the organic solution (b) bottom surface of polyamide facing MPD aqueous solution and (c) cross-section of the polyamide. For (a) and (b), the polymer was synthesised with 0.1 w/v % TMC and 2 w/v % MPD and reacted for 6 days. For (c) the polymer was synthesised with 0.05 w/v % TMC and 2 w/v % MPD and reacted for 2 days.

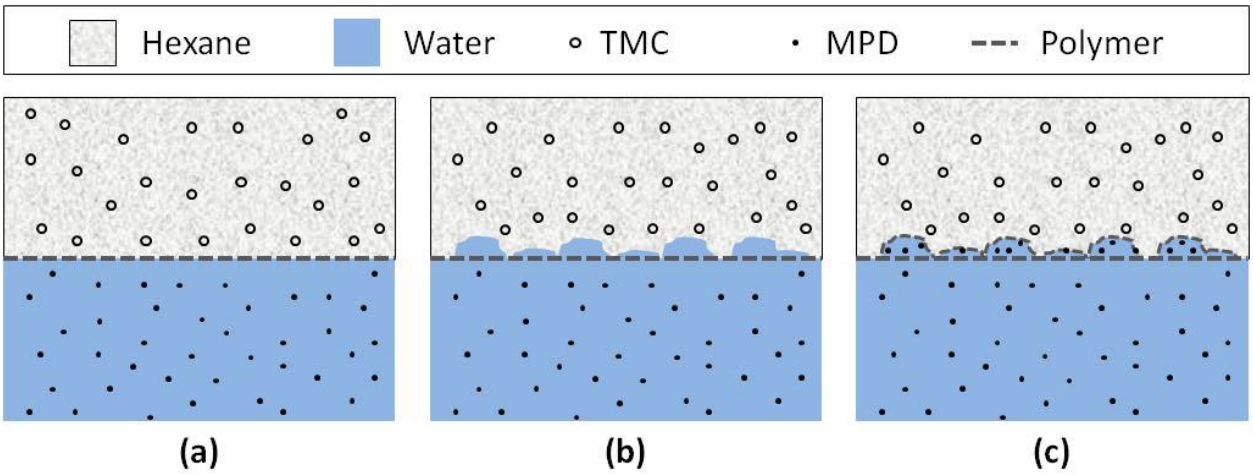

Figure 5: An illustration of the mechanism of thick membrane formation: (a) initial thin membrane formation upon contact with the two solutions (b) slow diffusion of water through the membrane (c) diffusion of MPD through the membrane causing new membranes to form.

(a)

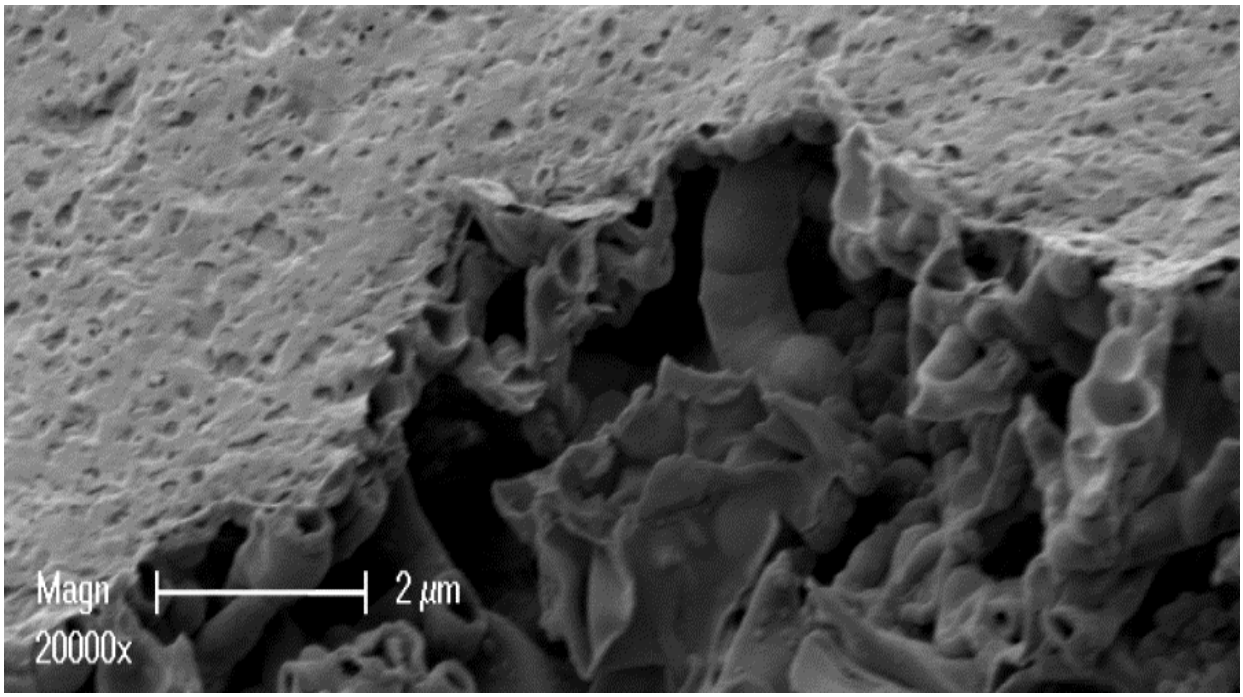

(b)

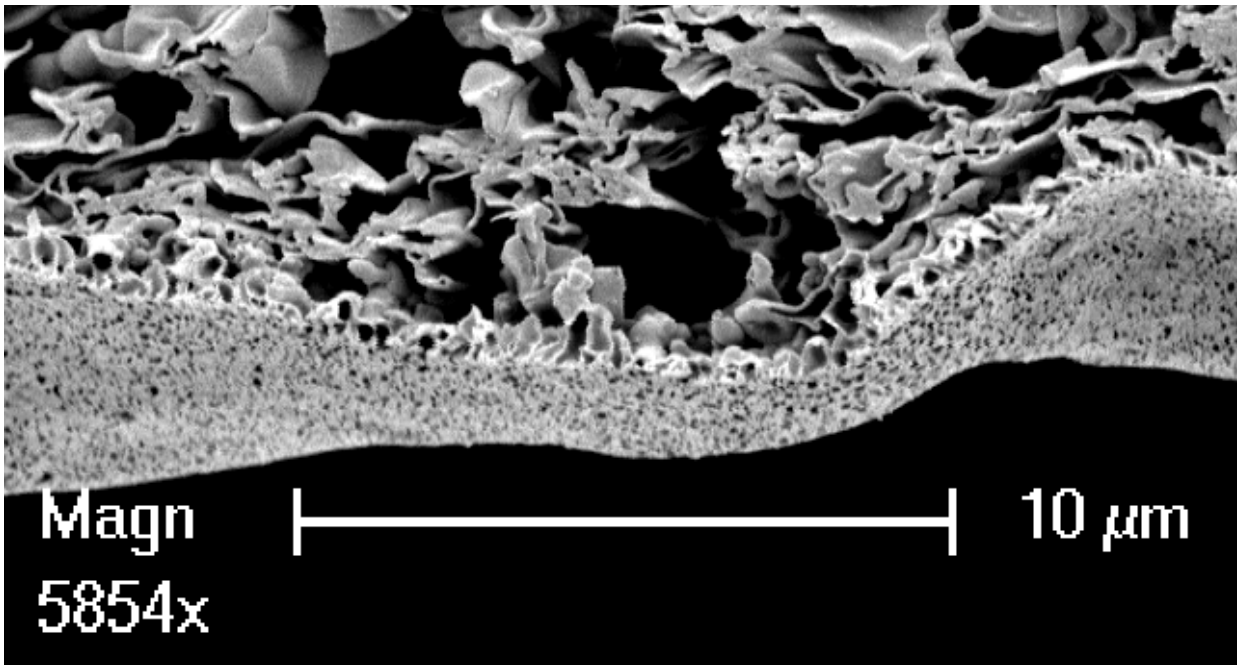

Figure 6: SEM images of (a) the surface facing the aqueous side with the subsurface exposed and (b) enlarged image of the cross-section of the film barrier facing the aqueous side.

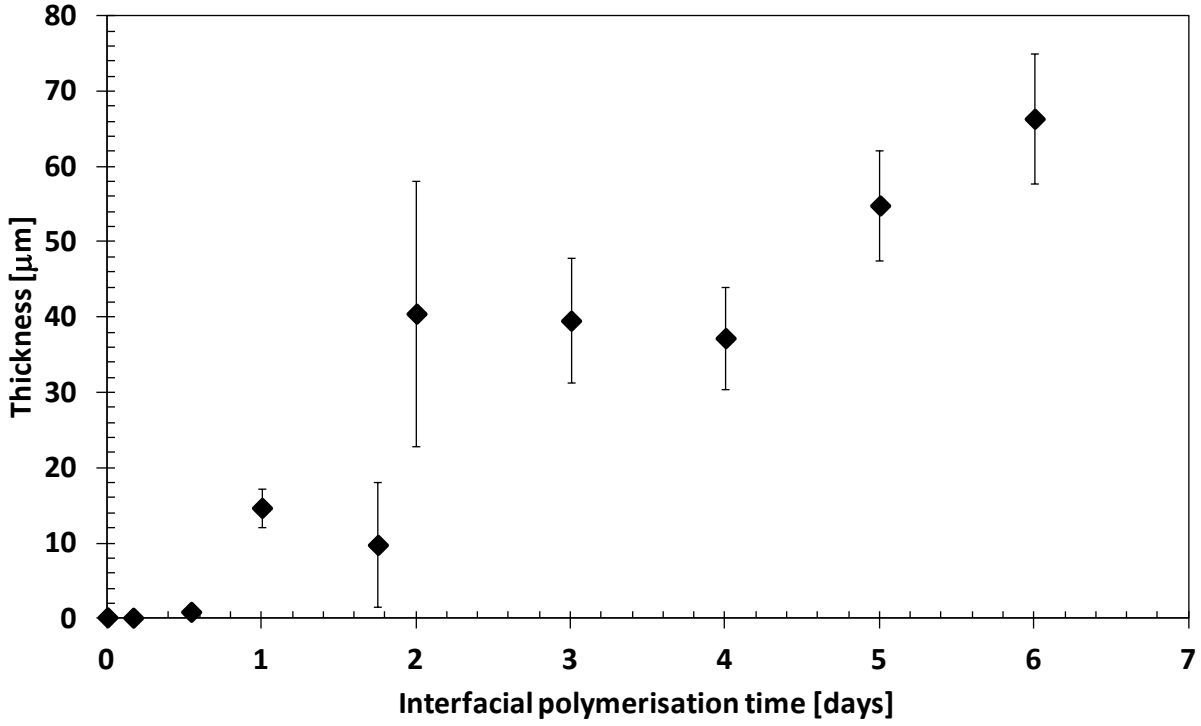

Figure 7: Polymer film thickness as a function of polymerisation time. The MPD and TMC concentration was fixed at 2 w/v% and 0.1 w/v%, respectively.

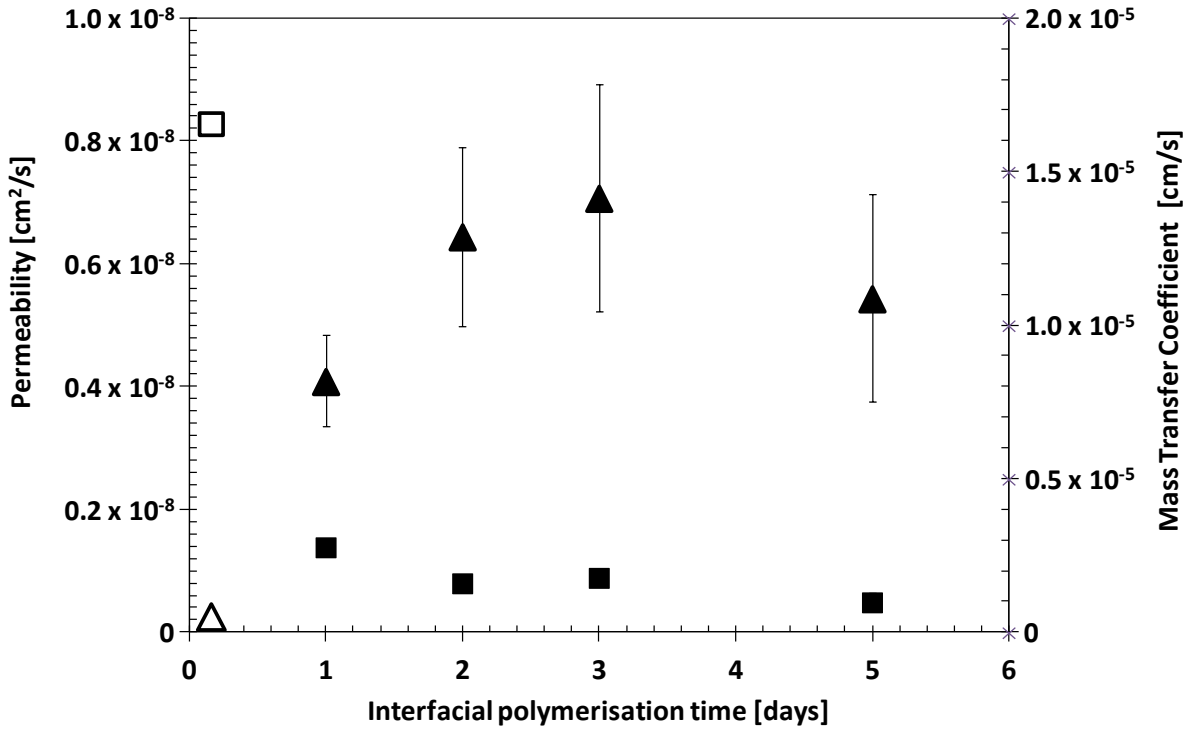

Figure 8: Salt permeability (triangles) and salt mass transfer coefficient (squares) as a function of polymerisation time. The thick polyamide membranes were made with a fixed concentration of 2w/v% MPD and 0.1 w/v % TMC. The empty symbols are thin polyamides made on top of polysulfone supports, similar to commercial TFC membranes.

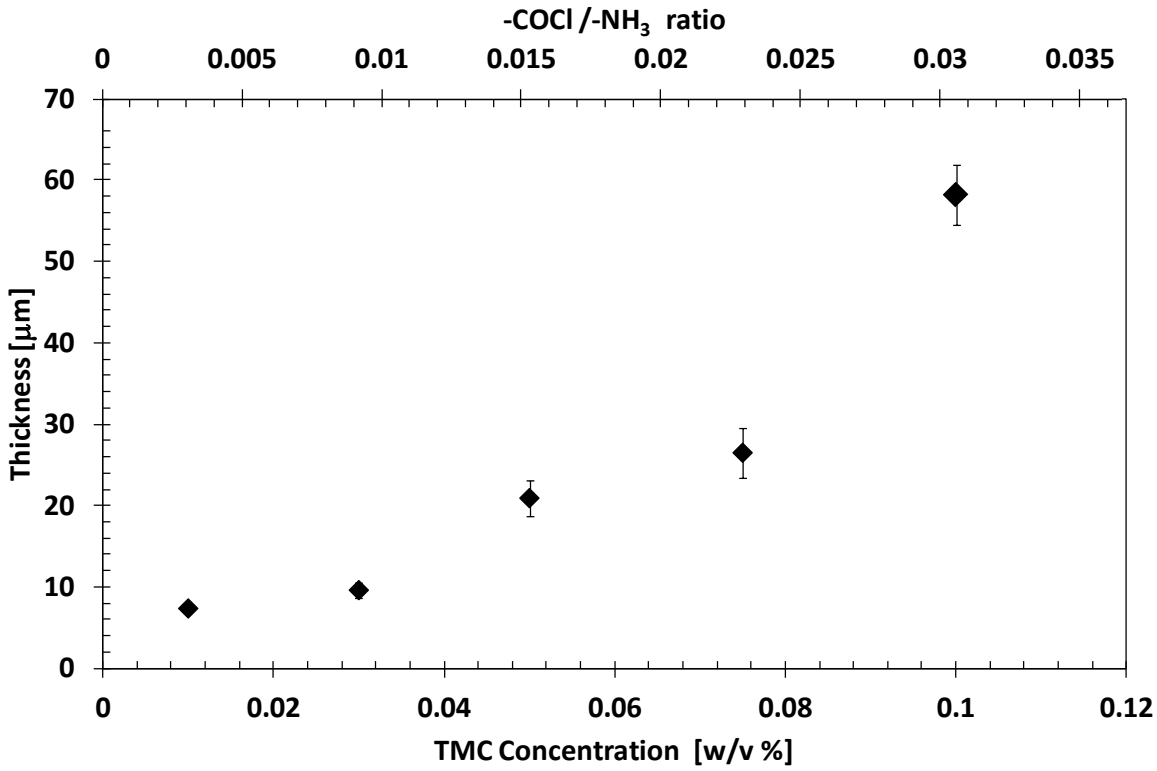

Figure 9: Polymer film thickness as a function of TMC concentration as well as the -COCl/-NH3 ratio. The polymerisation reaction time and MPD concentration was fix at 2 days and 2w/v%, respectively.

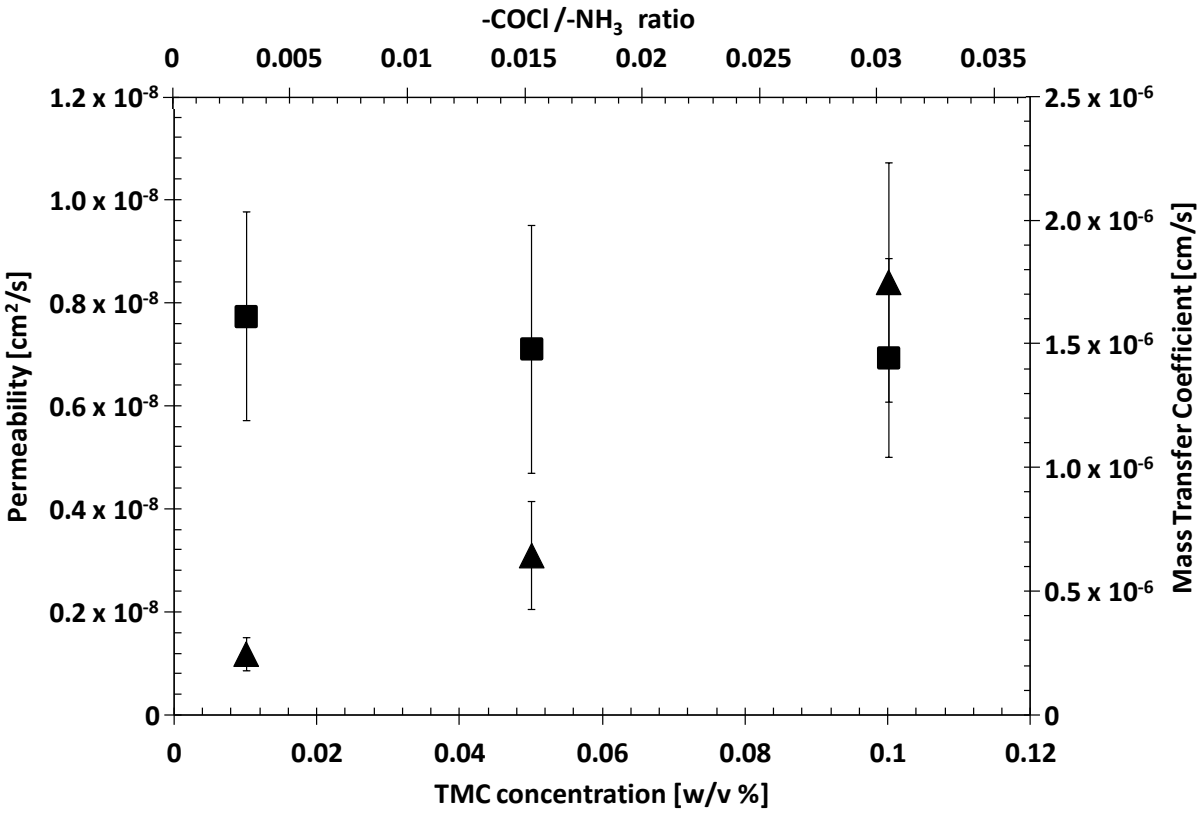

Figure 10: Salt permeability (■) and salt mass transfer coefficient (▲) as a function of TMC concentration as well as -COCl/-NH_3 ratio. The polymerisation reaction time and MPD concentration was fix at 2 days and 2w/v%, respectively.

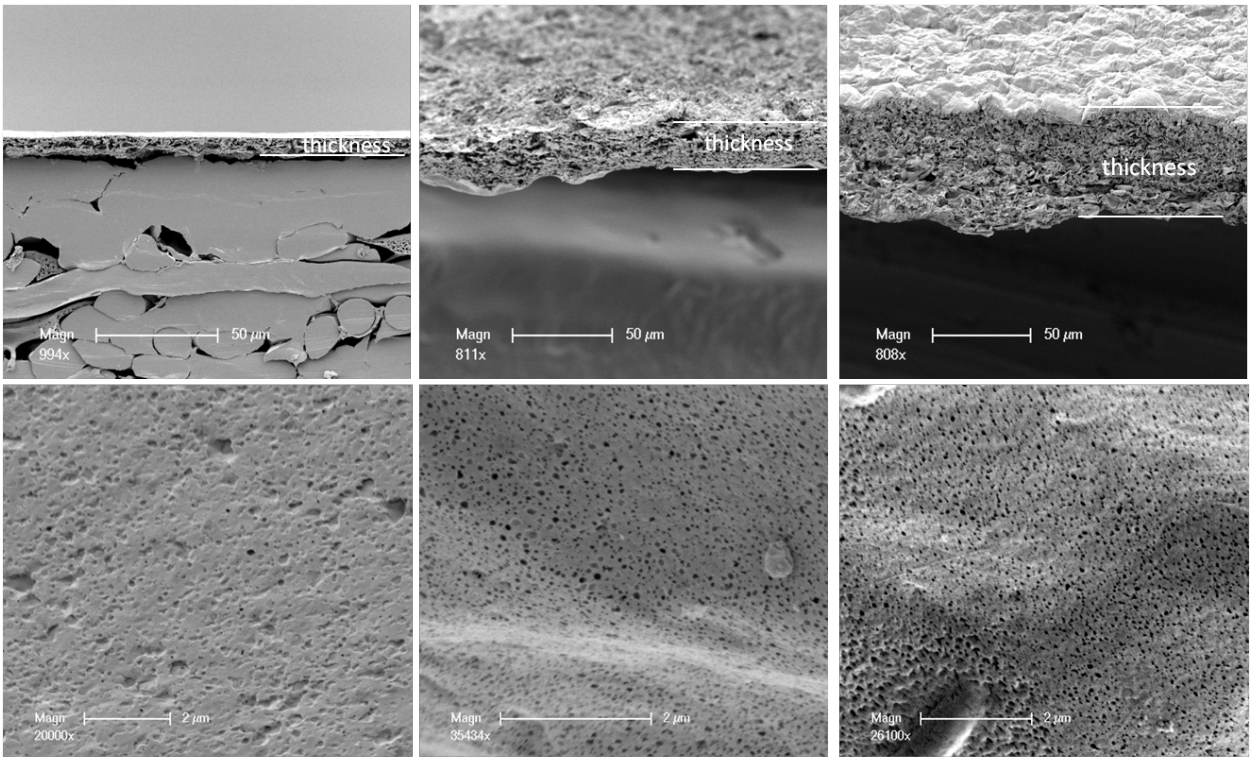

Figure 11: SEM image of aromatic polyamide showing the cross-sectional thickness (top) and surface facing the MPD aqueous phase (bottom) synthesised with different concentrations of TMC: (a) 0.01 w/v % (b) 0.05 w/v % and (c) 0.1 w/v %. The aqueous phase was fixed at 2 w/v % MPD and the interfacial polymerization time was 2 days. In (a) the polyamide membrane is too thin to be self supporting and therefore for the cross-sectional image, the membrane is rested on top of a polyester support for imaging purposes.

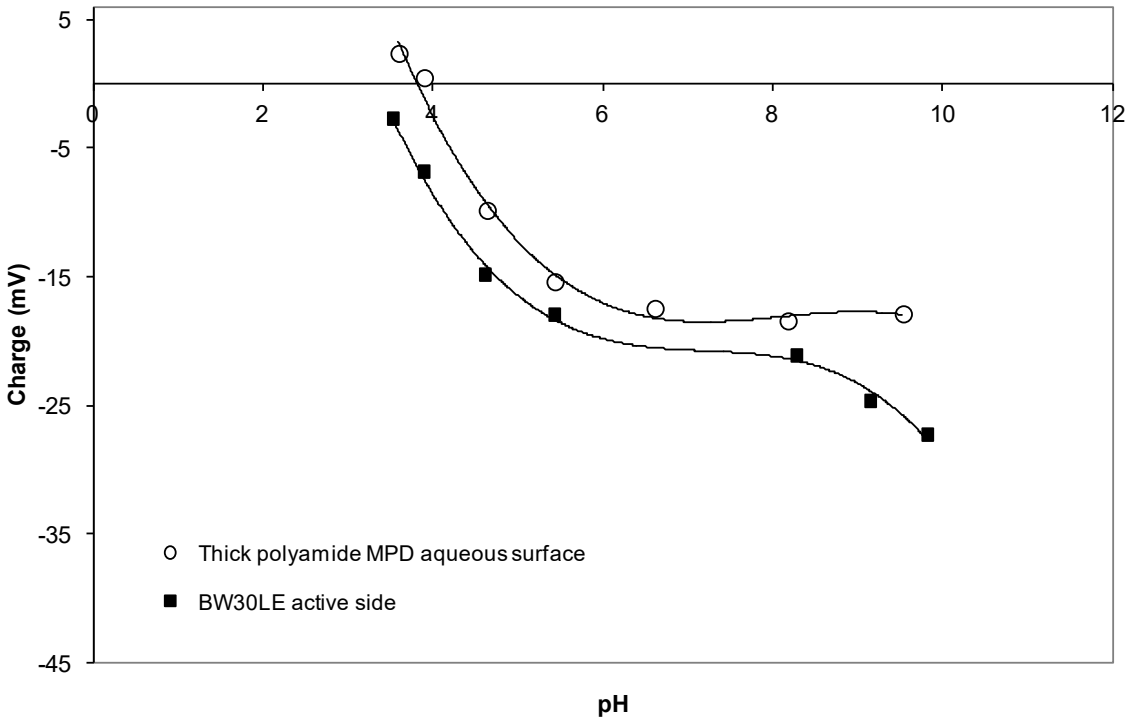

Figure 12: Surface charge measurements for the membrane surface facing the MPD aqueous side (circle) and for the surface facing the TMC organic side (square), as a function of pH.